https://doi.org/10.31713/m1204

# GEOMECHANICS INFLUENCE ON MINING BLOCKS IN SEISMICALLY ACTIVE AREAS AT MUFULIRA MINE DEEPS SECTION

**Dr. Victor Mutambo**

Head of Department. Department of Mining Engineering, School of Mines, University of Zambia, Lusaka, Zambia

**Moses Mukuka**

MSc., Mining Geologist, School of Mines, University of Zambia, Lusaka, Zambia



**Abstract**

Mufulira mine has been in operation since 1933. The mine is situated on the copperbelt region of Zambia. It is predominantly rich in copper and cobalt mineralization. Due to increase in mine depth that currently stands at 1,557m, the mine has been experiencing geomechanical challenges such as rock failures due to excessive stress changes around some mining blocks. This has necessitated changes in mining sequences to suit the present geomechanical conditions such as development of de-stressing cross-cuts between 62 and 64 blocks. Additionally, blocks have been subjected to shotcrete support method to prevent possible rockbursts/rock falls which can endanger safety of men working in these areas.

This study applied geotechnical investigation and geological field mapping methods to understand the Geomechanics mechanisms controlling the rock burst prone mining blocks at Mufulira mine. Damage mapping conducted in the footwall drives, cross-cuts and mining drives excavations indicate that there is a changing stress loading as one moves away from the retreating stope face to the east. The rockmass damage predominated by spalling process usually initiates from the northern top corner of the excavation drive.

## 1. Introduction

According to Suorineni F. T. (2013), geomechanics has proven to be the backbone of safe and cost effective mining practice. However, experience shows it still does not have the appreciation of most mines until there is a fatality or costly ore sterilization. This lack of understanding has affected the growth and maturity of the subject of rock mechanics, a key component of geomechanics. In rocks, free surfaces rarely exist until fracture occurs through breaking the cohesive bonding in the aggregate of minerals! Thus, the strength of rocks is NOT a simultaneous mobilization of cohesion and friction but successive destruction of cohesion followed by mobilization of the frictional strength due to the presence of free sur-faces following the destruction of cohesion.

Martin (1993) showed that in massive, hard, brittle strong rock masses, maximum friction and maximum cohesion are not mobilized simultaneously as Mohr Coulomb equation suggests. By the time friction is fully mobilized a significant portion of the cohesion has been lost (Fig. 1).

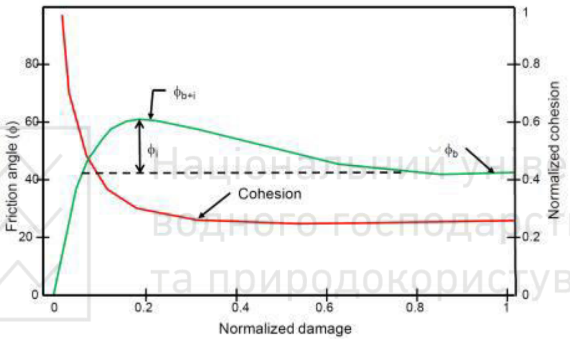



**Fig. 1.** Cohesion Loss-friction Mobilization (After Suorineni F. T., 2013)

$$\sigma'_1 - \sigma'_3 = \sigma_{ci}\sqrt{\frac{m\sigma'_3}{\sigma_{ci}} + s} \qquad (1)$$

$$\sigma_1 - \sigma_3 = \frac{\sigma_{ci}}{3} \qquad (2)$$

Where $\sigma_1$ and $\sigma_3$ are the induced major and minor principal stresses, and $\sigma_{ci}$ is the uniaxial compressive strength of the intact rock. Equation (2) implies that massive strong brittle rocks friction plays have very little role in their failure. Note that Equation It should be noted that was equation (2) was based on tests and observations made on granite rock. Suorineni *et al*. (2009) showed that Equation (2) is rock-type de-pendent, and could be written as follows

$$\sigma_1 - \sigma_3 = A\sigma_{ci}, \qquad (3)$$

where A is a rock type dependent parameter.

According to Ben-Guo *et al*. (2015), the mechanism of rock burst are due to strain relaxation of surrounding rock mass in newly excavated areas, and the dynamic response of rock mass to blast induced waves. Part of the strain energy stored in highly stressed zones is released in the form of shear movements along weak planes of discontinuities, while the other part of it is converted into kinetic energy, which eventually leads to rock expulsion from the surface of an excavation. Kaiser and Cai (2012) categorized rock burst damage in three classes: bulking due to fracturing, Ejection of rock due to seismic energy transfer, and rock fall induced by seismic vibration.

There are several methods of monitoring and identifying potential rock burst-prone zones. Research and industrial practice on the estimation and identification of rock burst-prone zones mainly focuses on theoretical analysis, laboratory test, numerical simulation and field measurement, as proposed by Fei *et al*. (2018). Field measurement includes the use of a micro-seismic monitoring system and field geological structural mapping.

This study applied geotechnical investigation, uniaxial compression tests and geological field mapping.

**2. Mufulira mine DEEPS section-Case Study**

**2.1 Site Description**

Mufulira mine is located in the Copperbelt province of Zambia in Mufulira town. The mine lies on latitude 12° 32' 22" South and longitude 28° 14' 10" East. The mine is one of the biggest underground mines in Zambia, and its major product is copper. The license area for Mufulira mine consists of Mufulira West Portal, Mufulira East Portal and the main Mufulira mine which comprises the upper, central and deeps section. This research is being conducted on the main Mufulira mine, deeps section. ploys Mechanized Continuous Retreat (MCR) mining method, which is a variant of sublevel open stoping. Fig. 2 shows a typical layout of Mechanized Continuous Retreat mining method. The method involves fan drilling of long holes from the roof of a sublevel. The sublevels are spaced at intervals of 17 m.

The layout of the mine consists of access crosscuts from the decline to the orebody. At the end of these access crosscuts, a footwall drive is developed, as illustrated in Fig. 2*d*. The footwall drive and the mining drive are linked by multiple orebody crosscuts, which are spaced at 50 m apart in the mining level (drilling level) as shown in Fig. 2*b*. However, at the drawing level, where blasted ore is collected from, as shown in Fig. 2*d*, the orebody crosscuts are spaced at 25 m apart. In terms of dimensions, the mining drive, footwall drive and crosscuts are all 4 m in height and 4 m in width.

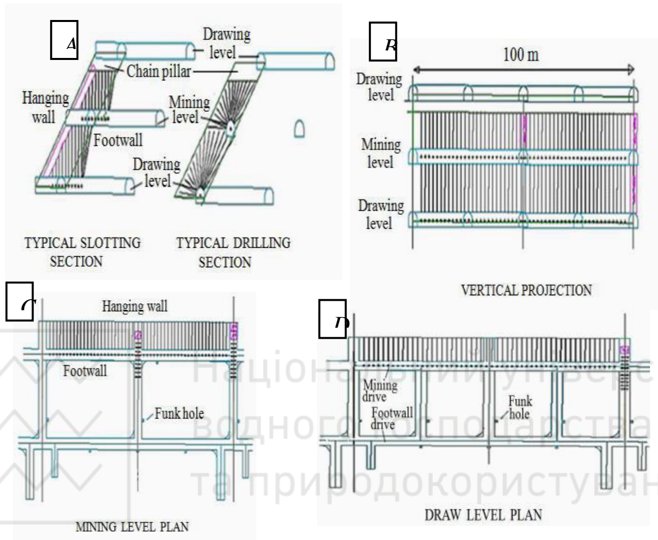


**Fig. 2.** Typical variant of MCR Mining method at Mufulira mine

If fan drilling is performed on two sublevels and the blasted ore is collected from the bottom sublevel, which is referred to as drawing level, then the method is known as Mechanized Continuous Retreat 2 (MCR2). If both fan drilling and ore collection are performed only on one sublevel, then the method is known as Mechanized Continuous Retreat 1 (MCR1). The design of the stope leaves a 3 m pillar at the roof as indicated in Fig. 3), which is known as the chain pillar. According to Immanuel and Mutambo (2016), the purpose of the chain pillar is to retain the broken hanging wall material from upper levels and thus prevents ore dilution to the blasted ore.

**2.2. Geology of the rock burst prone mining blocks**

The major geological units comprise a series of five different units. Stretching from south-west to north-east of Mufulira mine, these units are; basement complex, footwall quartzite, mineralized series, the hanging wall formation and finally the carbonate rocks. The mineralized series hosts three orebodies of Mufulira mine, *A*,*B* and *C* orebody.


**Fig. 3.** Showing Bornite(dark blue) & Chalcopyrite(yellow) mineralised C - Quartzite(C-Orebody) from 61P5 1523 mL; (A) Longitudinal 49 mm diameter core sample, ( B) Cross-sectional view of the 49 mm core sample, (C) Thin section of the C-Orebody sample

The orebodies are bedded or of stratiform type (Brandit, 1962). Location of the rock burst prone area extends from 61 block up to 65 block, which ranges from footwall drives through cross-cuts and mining drives. All the three orebodies dip at an average angle of 45º. The footwall ranges in thickness from 0 to 5,0 m. Table 2 shows the general stratigraphy and geotechnical characteristics in Mufulira DEEPS section.

Table 2

General Stratigraphy and Geotechnical Characteristics in Deeper Mining Area

| Geological unit | Thick | UCS (MPa) | RMR | General Geotechnical Description |
|---|---|---|---|---|
| Lower argillaceous quartzite | 40 m | 320 | | Good quality, massive, bedded partings infilled with Calcite. |

| | | | | |
|---|---|---|---|---|
| A' orebody quartzite | | 220 | 81 | Good quality, but bedded with weak graphitic partings in lower, grey, vacke part of orebody. Upper part shows calcite infilled bedding partings with beds 10 to 50 cm thick. |
| InterA/B quartzite | | 320 | 68 | Average quality, Bedded |
| Banded shales, quartzite and dolomite | | 130-250 | | |
| Lower dolomite | | 50 | 49 | Weak and friable |
| B' orebody quartzite | 7 m | 320 | 81 | Very good quality, bedded. |
| Inter B/C quartzite | 4-18 m | 310 | 64 | Good quality, bedded |
| Banded shales& dolomites | | 211 | | Moderate quality. Mud seam at base may be weak in places. |
| 'C' orebody quartzite | 9 m | 310 | 81 | Very good quality |
| quartzite | 0-150 m | 270 | 61 | Shear zone at basement contact |
| Basement Schist | | 300 | | Strong competent |
| Basement Quartzite | | 300 | go | Very strong competent |

## 3. Materials and Methods

Geotechnical investigation, uniaxial compression tests and geological field mapping were undertaken in the seismically active zones in order to understand the geological characteristic of the rock type in the study area.

The Rock Mass Rating (RMR) parameter for orebody and hangingwall rocks was determined according to Laubscher's (1990) Geomechanics classification. RMR parameters were based on the measurement of discontinuity sets (number and spacing) as well as the character of the discontinuity. The RMR was then combined with the intact rock strength to give the overall Rockmass Strength Rating. Map3D

Boundary Element Method and examine 2D were used to model the tresses.

## 4. Results and Discussion

From the images, the C orebody quartzite showed coarse-grained (arkosic) sandstone severely disturbed and poorly sorted, with the ore forming minerals identified as chalcocite, chalcopyrite and Bornite. The footwall quartzite (Fig. 4) showed characteristics of granular to grained (arkosic) sandstone, which is poorly sorted with weak contacts that are metamorphosed.

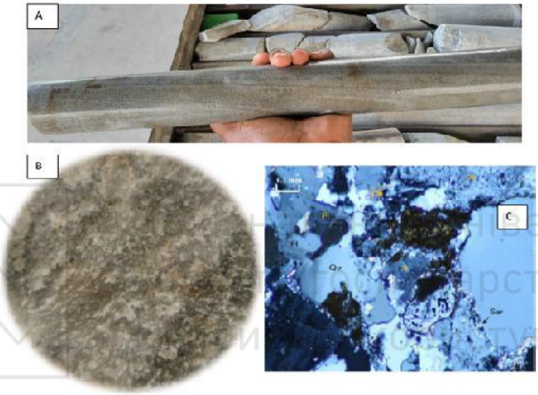


**Fig. 4.** Showing fresh footwall quartzite core sample from 61P5 1523 mL; (A) Longitudinal 49 mm diameter core sample, (B) Cross-sectional view of the 49 mm core sample, (C) Thin section of the footwall quartzite sample(*Qz*: Quartz, Pl: Plageoclase, Ser: Sericite, Cb: Carbonate mineral)

Some of the minerals observed in the footwall quartzite included quartz, orthoclase, plageoclase, spinel and granite. In both the orebody quartzite and footwall quartzite, sericite and anhydrite were identified as secondary minerals.

### 4.1 Geotechnical setting

#### 4.1.1 Rock structure system

On the scale of the dimensions of the mine opening, the Mufulira mine rockmass is generally massive and strong. The rockmass exhibits a transition in the behaviour from brittle to ductile as one moves from the west to the east.

The eastern fringe is usually highly weathered and blocky in many places. In general the present geological discontinuities are moderately to highly persistent, with wide to very wide spacing. Discontinuity surfaces tend to be smooth to slightly rough on the scale of several centimetres and planar on the scale of several metres. Infillings are I rare within the orebodies, but can occur frequently in the footwall quartzites. Discontinuities are usually dry except for areas in the eastern fringe where water seepage along discontinuities can occur and iron staining is common. The footwall quartzite is characterised by beddings and cross-bedding planes. Bedding planes are the result of disturbances in the sedimentation process and are characteristic for all types of sedimentary rock, particularly mechanical sediments. These are very common on the east and towards the eastern fringe. Their interaction with other discontinuities under a high stress environment creates block instability around excavation openings.

Schistose occurrences are also occasionally present in the basement and footwall quartzite formations. Schistocity planes are typical in most metamorphic rocks. During metamorphism, mineral grains are rearranged resulting in a predominant mineral grain orientation due to rock pressure. Thus, weakness planes are generated especially if such planes are formed by mica or other lamellar minerals. Pressure release and/or tectonic activity can open such planes. As opposed to bedding planes, schistocity plane surfaces are mostly rough or undulating. If schistocity planes have opened throughout the metamorphic process, they are often filled with hydrothermal quartz and occasionally carbonates.

The field discontinuity survey on the levels from 1357 mL to 1457 mL were conducted. The results and analysis of the survey are presented below

The results of the geotechnical discontinuity survey reveal three (03) major discontinuities which create potential unstable wedges (Fig. 5) when exposed in the footwall drive or the crosscut excavation backs/walls. The geometrical and surface properties of the major discontinuities are presented in the Table 1.

Table 1

Geometrical and surface properties of the major discontinuities

| Discontinuity code | Dip (°) | Dip Direction(°) | Persistence | Spacing mm | Planarity | Aperture mm | Roughness | Fill |
|---|---|---|---|---|---|---|---|---|
| J | 43 | 023 | 3-10 | 60-200 | P | 0,1-0,25 | R | Nil |
| J | 72 | 283 | 3-10 | 200-600 | P | 0,1-0,25 | R | Nil |
| J | 40 | 271 | 3-10 | 200-600 | P | 0,1-0,25 | S | Nil |

Key;
Roughness; *R*-rough, *S*- smooth, *SL* - slicken-sided
Planarity; *P*-planar, *W*-wavy, *I*-irregular, *J*-Joint

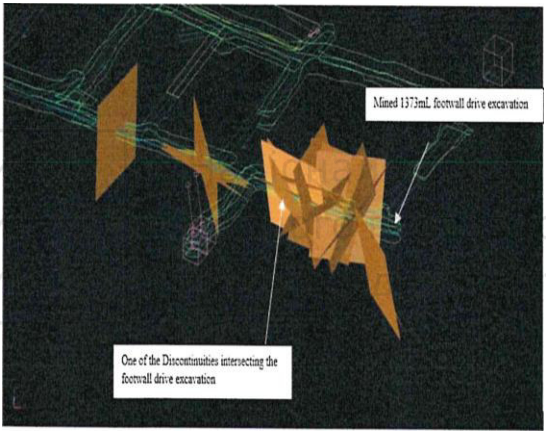


**Fig. 5.** Photo depicting 3D Surpac model of discontinuities intersecting the drive

### 4.1.2 Rock mass mechanical properties

According to the classification system used by the International Society for Rock Mechanics (ISRM - 1986 Rock Characterisation; Testing and Monitoring), the orebody quartzite are described as Extremely STRONG while the footwall and the hanging wall rocks are STRONG to Very STRONG.

The exception is the lower dolomite unit which forms the immediate hanging wall of the B orebody and is classified as Medium STRONG to STRONG. The approximate uniaxial compressive strengths and the Rock Mass Ratings (RMR) of the Mufulira mine rocks are given below; they were derived from point load tests.

The footwall quartzite in which most of the secondary development is placed, has a uniform strength except the eastern side of 64-Block where it is severely leached (a weathering effect) resulting in variable rock strengths between LOW to Very STRONG. The rockmass formation in the orebody between 60 and 64 blocks is strong and brittle.

This is the part of the mine were brittle fracturing and bulking dominates the rock mass failure process.

Violent rockmass failures mostly triggered by during primary stope blasting have been experienced in the 60 to 64 blocks orebody formation.

### 4.1.3 Rockmass rating and classification

The orebody rocks can be classified as Good to Very Good, the Lower dolomites as Fair and the footwall quartzite from 50 to 64 Blocks as marginally GOOD.

The occasional presence of joint planes in the footwall quartzite infilled with calcite or anhydrite combined with the unfavourable orientation of bedding planes with respect to footwall drives makes this unit particularly susceptible to wedge failures.

East of 64 Block is classified as Fair, locally and occasionally becoming poor where unfavourable discontinuity orientations occur in combination with wet, moderately weathered weak rock.

### 4.1. Mine Stress Regime

In 1976, the Mine at the time conducted some stress measurements. These 'premining' stress measurements were conducted on the 810 mL by overcoring six largediameter rosettes that were located around the circumference of a bored raise.

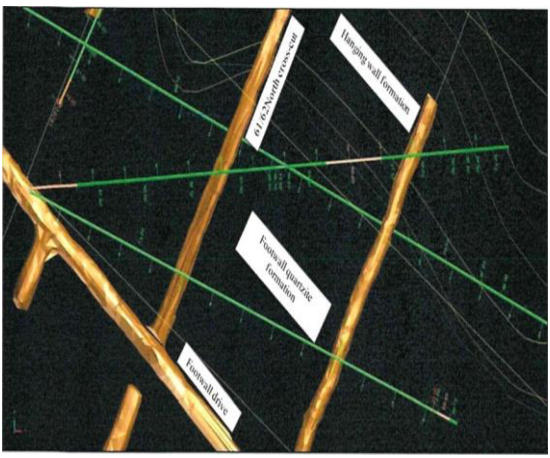

**Fig. 6**. Level plan on 1473 mL showing distribution of RMR along the drilled holes (Predominantly Good rockmass conditions)

Table 3

Laubscher's Rock Mass Strength (RMS) rating of the Mufulira rock formation

| Rock type | Rock mass strength (RMS) MPa | Class |
|---|---|---|
| Footwall quartzite | 112 | Good |
| C-quartzite | | GIV Good |
| Inter B-C | 94 | Good |
| B-quartzite | | GIV Good |
| Lower dolomite | 15 | FAIR |
| Inter A-B | 126 | Good |
| A-quartzite | 164 | GIV Good |

The measurements obtained showed that the principal stresses some 200 m down-dip of mining were as presented in Table 4.

Table 4

Magnitude and orientation of principal stresses from over-coring data results (Broome & Sandy, 1976)

| | Magnitude | Orientation (dip/direction, degrees) |
|---|---|---|
| Sigma 1 | 37,1 MPa | 72/345 |
| Sigma 2 | 16,1 MPa | 17/192 |
| Sigma 3 | 11,6 MPa | |

In 1984 and 1985, more stress measurements were taken by making use of five SCIRO cells. These cells were installed in the 50-51 drainage crosscut on 1032 m. Several problems were encountered, and as a result only one of the tests was successful. The major principal stresses for this test may be seen in the Table 5.

Table 5

Magnitude and orientation of principal stresses from SCIRO cells results (Broome & Sandy, 1987)

| | Magnitude | Orientation (dip/direction, degrees) |
|---|---|---|
| Sigma 1 | 37,8 MPa | 61/299 |
| Sigma 2 | 34,1 MPa | 17/176 |
| Sigma 3 | 23,6 MPa | 23/078 |



The orientation of both tests were plotted on a stereonet in order to assess and compare the results as shown in Fig. 7.

The ore extraction method employed at Mufulira mine (DEEPS section) is associated with high stope-induced abutment stresses. Generally the ore body dips at about 45 degrees and it is deduced from field observations of break-outs on the excavation boundaries that the major principal stress is oriented perpendicular to the dip of the ore body, whilst the minor and intermediate stresses are oriented along dip and strike of the ore body respectively.

Damage mapping conducted in the footwall drives, cross-cuts and mining drives excavations indicate that there is a changing stress loading as one moves away from the retreating stope face to the east.

The rockmass damage predominated by spalling process usually initiates from the northern top corner of the drive excavation, see Fig. 7.

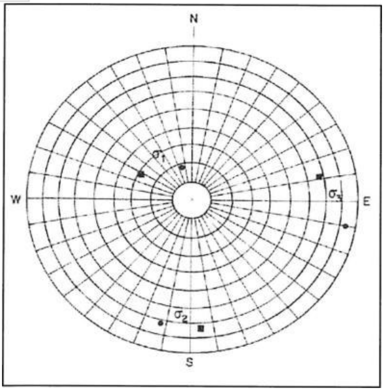


**Fig. 7.** Orientations of principle stresses obtained in 1976 (circles) and 1985 (squares), from Broome & Sandy, 1987 - showing good correlation between the two test results

As the location of the observed stress-induced damage is usually expected to be a function of the orientation of the major principal stress, it is deduced that the major principal stress is oriented perpendicular to the dip of the ore body, with the minor and intermediate principal stress oriented along dip and strike respectively. This to some extent verifies the results of the stress measurement conducted initially. The calibrated stress model constructed using Map3D Boundary Element Method software reproduces excavation model conditions that correlate very well with the observed/assumed conditions.

The model thus, is suitably used as a predictive tool to map out potential overstress zones. A 2D stress model using Examine-2D (Rocscience product) reproduced similar results, see Fig. 8.

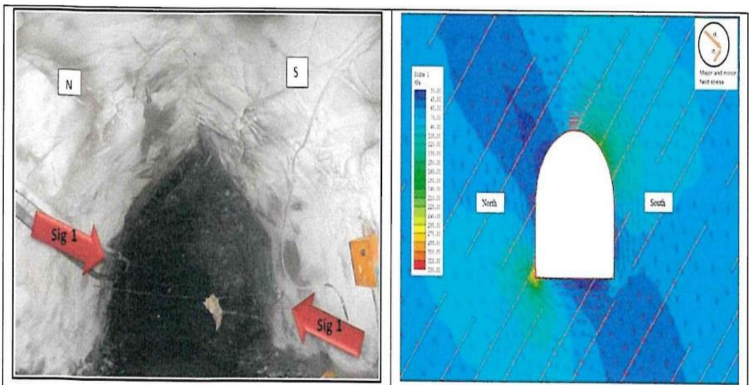


**Fig. 8.** Examine2D model; (A) showing the major principal stress orientation in Mufulira underground mine stress model and (B) showing stress results clip for induced stress field around the drive excavation

### 4.2. Rockmass condition in the affected blocks

Similar to the conditions in the existing cross-cuts, adverse ground conditions are anticipated at about 20 m before footwall contact of the C-orebody.

The targeted area for de-stress is located in extremely high stress environment with major principal stress exceeding 100 MPa in many places. Fig. 9 shows snapshots of Map3D display of major principal stress results contours.

The existing remains of the mining drive show that severe damage concentrated more on the southern side than the north and the roof.

This makes the method of holing into the void more practical as the fall-out depth into the roof does not exceed 3 m.

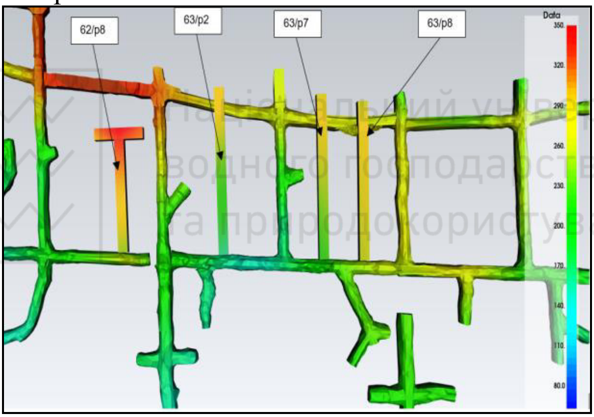


**Fig. 9**. Display of the tangential stress (cross-cuts will be mined from fair to adverse rockmass conditions – Tangential stress >250)

## 5. Conclusion

The orebody rocks in the DEEP section can be classified as Good to Very Good, the Lower dolomites as Fair and the footwall quartzite from 50 to 64 Blocks as marginally Good.

The occasional presence of joint planes in the footwall quartzite infilled with calcite or anhydrite combined with the unfavourable orientation of bedding planes with respect to footwall drives makes this unit particularly susceptible to wedge failures.

The ore extraction method employed at Mufulira mine (DEEPS section) is associated with high stope-induced abutment stresses.

Damage mapping conducted in the footwall drives, cross-cuts and mining drives excavations indicate that there is a changing stress loading as one moves away from the retreating stope face to the east.

The rockmass damage predominated by spalling process usually initiates from the northern top corner of the drive excavation.

Results of the simulation of the expected field stress conditions Map3D stress model indicates potential extensive damage in the 62P8 cross cut and drive and damage of the 63/p2 cross-cut after a few metres from the footwall drive. The conditions in 63/p7 and 63/p8 are expected to be fair (standard ground support) until about 30 m from the footwall drive.

**Acknowledgement**

The authors would like to thank management of Mopani copper mine for allowing this study to be undertaken at the mine site. Special thanks go to the Dean, School of Mines for providing logistical support.

**Potential Conflict.**

There is no potential conflict associated with this study.



*References*

1. **Long An, Changyu Jin, Dong Liu, Chenggong Ding & Xinghang Dai** (2018) Mechanism of core discing in the relaxation zone around an underground opening under high in situ stresses. Bull Eng Geol Environ 77, 1179–1189.

2. **Sinkala, P., Nishihara, M., Fujii, Y., Fukuda, D. and Kodama, J. & Chanda E.** (2019) Investigation of Rockburst in Deep Underground Mines, A case study of Mufulira mine, Copperbelt, Zambia. ARMA, American Rock Mechanics Association. 3:6-10

3. **Kaiser, P.K. and M. Cai**. 2012. Design of rock support system under rock burst condition. Journal of Rock Mechanics and Geotechnical Engineering. 4 (3): 215– 227.

4. **Sheng-Jun, M., C. Mei-Feng, G. Qi-Feng and H. Zheng-Jun.** 2016. Rock burst prediction based on in-situ stress and energy accumulation theory. International Journal of Rock Mechanics and Mining Science. 83:86–94

5. **Tian-Hui, M., T. Chun-An, T. Shi-Bin, K. Liang, Y. Qun, K. De-Qing and Z. Xu**. 2018. Rockburst mechanism and prediction based on micro-seismic monitoring. International Journal of Rock Mechanics and Mining Science. 110:177–188.

6. **Manchao, H., X. Hongman, J. Xuena, G. Weili, Z. Fei and L. Kangyuan.** 2012. Studies on classification, criteria and control of rockbursts. Journal of Rock Mechanics and Geotechnical Engineering. 4(2): 97– 114.

6. Suorineni F. T. (2013), "Geomechanics Challenges and its Future Direction – Food for Thought", Ghana Mining Journal, pp. 14 - 20.

7. **Crouch, S.L.** (1976). Analysis of stress and displacements around underground excavations: an application of the displacement discontinuity method. Tech. Rep., Department of Civil and Mineral Engineering, University of Minnesota.

8. **Kristoffer B. & Daniel G.** (2014), 'Challenges with deep mining, Case studies at Mindola and Mufulira underground mines, Zambia' pp. 15-50.

9. **Siyanda B.** (2015). Integrated petrographic, geomechanical and seismological studies of rockmass behaviour during the extraction of the Cooke 4 shaft pillar. PP. 29-67

10. **Fei, L., M. Tianhui, T. Chun'an and C. Feng.** (2018). Prediction of rockburst in tunnels at the Jinping II hydropower station using microseismic monitoring technique. Journal of Tunnelling and Underground Space Technology. 81:480–493.

11. **Ng'ambi, I and Mutambo, V.** (2016). Optimization of stope recovery and dilution at Mufulira mine through application of appropriate designs and practices. International Journal of Applied Research. 2(9). 397-402.

12. **Brandit, R. T.** (1962). Relationship of mineralization to sedimentation at Mufulira, Northern Rhodesia. Institution of mining and metallurgy. Vol. 71, 459-479.

13. **Hudson, J.A. and J. P. Harrison** (2000). Engineering Rock Mechanics: part 2 illustrative worked examples. Elsevier Science Ltd: Oxford, 95-109.

14. Zhang, L. and H. H. Einstein (2004). Using RQD to Estimate the Deformation Modulus of Rock Mass. International Journal of Rock Mechanics and Mining Science. Vol. 36, No. 5, 337-342.

15. **Alam, B.A.K.M., M. Niioka, Y. Fujii, D. Fukuda and J. Kodama** (2014). Effects of confining pressure on the permeability of three rock types under compression. International Journal of Rock Mechanics and Mining Science. 65: 49-61.